Arab J Geosci (2015) 8:10015–10030
DOI 10.1007/s12517-015-1890-8

ORIGINAL PAPER

Site response assessment at the city of Al Khobar, eastern Saudi Arabia, from microtremor and borehole data

M. Alharbi[1] · M. Fnais[1] · A. Al-Amri[1] · Kamal Abdelrahman[1,3] · Meinrat O. Andreae[1,2] · M. Al-Dabbagh[1]

Received: 6 December 2014 / Accepted: 16 March 2015 / Published online: 3 May 2015

Abstract Al Khobar City is affected by distant earthquakes from the Zagros fold-fault belt, which is part of the subduction zone between the Arabian and Eurasian plates. These earthquakes have generated substantial site effects on the sedimentary layers, which in turn significantly influence earthquake ground motions in the area. Mapping of site response using microtremor measurements compared with geological and borehole data from Al Khobar City is the main objective of this work. The resonance frequency and the corresponding horizontal-to-vertical (H/V) ratio values have been calculated using the Nakamura technique on data from seismograph instruments deployed at 113 sites in Al Khobar City for different time periods. The recording length was about 1 h with a sampling frequency of 100 Hz. Most of the measured sites present three peaks of resonance frequency; the first peak ranges from 0.33 to 1.03 Hz, the second peak ranges from 1.03 to 1.23 Hz, while the third one ranges from 1.23 to 1.73 Hz. Tests have been conducted to ensure that these peaks are of natural origin The northern zones of Al Khobar City have lower resonance frequency values, indicating great sediment thickness. In contrast, the southern parts of the city have higher resonance frequency values, suggesting shallow bedrock depths. Furthermore, 29 geotechnical boreholes have been drilled to different depths in Al Khobar City. Standard penetration test (SPT) data has been corrected and used to calculate the resonance frequency at their locations. The borehole results showed that the resonance frequency values range from 0.27 to 1.95 Hz. These results are well correlated with those from the microtremor measurements. Accordingly, the first peak has been interpreted as being due to the impedance contrast between the limestone bedrock and the overlying sediments, while the third peak originates from a boundary between the uppermost surface layer and the underlying sediments.

Keywords Fundamental frequency · Microtremor · Boreholes and amplification

✉ Kamal Abdelrahman
ka_rahmaneg@yahoo.com

[1] Geology and Geophysics Department, King Saud University, Riyadh, Kingdom of Saudi Arabia

[2] Biogeochemistry Department, Max Planck Institute for Chemistry, Mainz, Germany

[3] Seismology Department, National Research Institute of Astronomy and Geophysics, Cairo, Egypt

Introduction

Al Khobar City lies in the eastern part of Saudi Arabia (Fig. 1), which includes numerous multinational projects. It is affected by distant earthquakes originating from active tectonics of the Zagros fold-fault belt, which represents one of the most seismically active belts (Al-Amri et al., 2008) where large earthquakes (M≥5) are quite common and have a potential for widespread damage. The local geology can significantly influence the scale and distribution of damages due to strong earthquakes. This, in turn, affects engineering structures such as petrochemical plants, tunnels, bridges, and high-rise buildings.

Local site response can be evaluated by different methods; however, it requires detailed geotechnical information about the materials through which the seismic waves propagate to the surface. Nakamura (1989) suggested a method that requires only one recording station. He proposed that site response could be estimated from the horizontal-to-vertical ratio of microtremors. This method has been tested and applied for

Fig. 1 Location map of Al Khobar City

several cities all over the world (Bard and Tucker, 1985; Lachet and Bard, 1994; Field and Jacob, 1995; Malagnini et al., 1996; Wakamatsu and Yasui, 1996; Safak, 1997; Konno and Ohamachi, 1998; Mucciarelli, 1998; Mucciarell et al, 1998, Fnais et al., 2010 and Al-Malki et al., 2014). Results obtained by implementing Nakamura's technique indicate that this method is one of the cheapest and most convenient techniques to reliably estimate resonance frequency (Bard, 2000).

Geological setting of the eastern province of Saudi Arabia

The surface geology of eastern Saudi Arabia is composed of consolidated and unconsolidated sediments (Fig. 2). The consolidated sediments are of Paleocene to middle Eocene and Miocene to Pliocene age, while the unconsolidated materials include Quaternary sabkha deposits, gravels, sands, and clays. According to Powers et al. (1963) and AlSayari and Zotl (1978), a sequence of continental and shallow marine coastal sediments extends along the Arabian Gulf with relatively low-relief terrain. The Upper Cretaceous and Eocene rocks are represented by limestone and dolomite, while Quaternary sequences are made from sandstone, sandy marl, and sandy limestone of non-marine origin. These sequences dip gently towards the east and northeast under the Zagros thrust belt.

Seismicity of eastern Saudi Arabia

As mentioned above, the active tectonics of the Zagros Thrust Fault represents the major earthquake prone area affecting the eastern province of Saudi Arabia. Convergence between the Arabian and Eurasian plates has led to the uplift of the Zagros Mountains and the Iranian Plateau, and makes this region one of the most seismically active in the Middle East (Al-Amri et al., 2008). The boundary is clearly delineated by teleseismic epicenters, although there are fewer epicenters south of Oman. Most earthquakes occur in the crustal part of the Arabian plate beneath the Zagros belt (Jackson and Fitch, 1981). Large earthquakes ($M \geq 5$) are distributed along this belt and reveal the potential for widespread damage from destructive earthquakes. The Zagros belt is a prolific source for large-magnitude earthquakes, with numerous events of magnitude $M \geq 7$ occurring in the last few decades. Unfortunately, only few seismological studies have been conducted in the eastern province of Saudi Arabia. However, based on the historical record, this province was subjected to a large earthquake ($5.8 \leq Mb \geq 6.2$) in 1832 AD (Ambraseys, 1988). According to Al-Shaabi (2004), about 69 instrumentally measured earthquakes ($2.4 < Ml < 5.8$) have occurred during the period of 1990–1998 in eastern Saudi Arabia (Fig. 3). Some of these events were due to the earthquake swarm in June–October 1994 and well correlated with the fault system in this area.

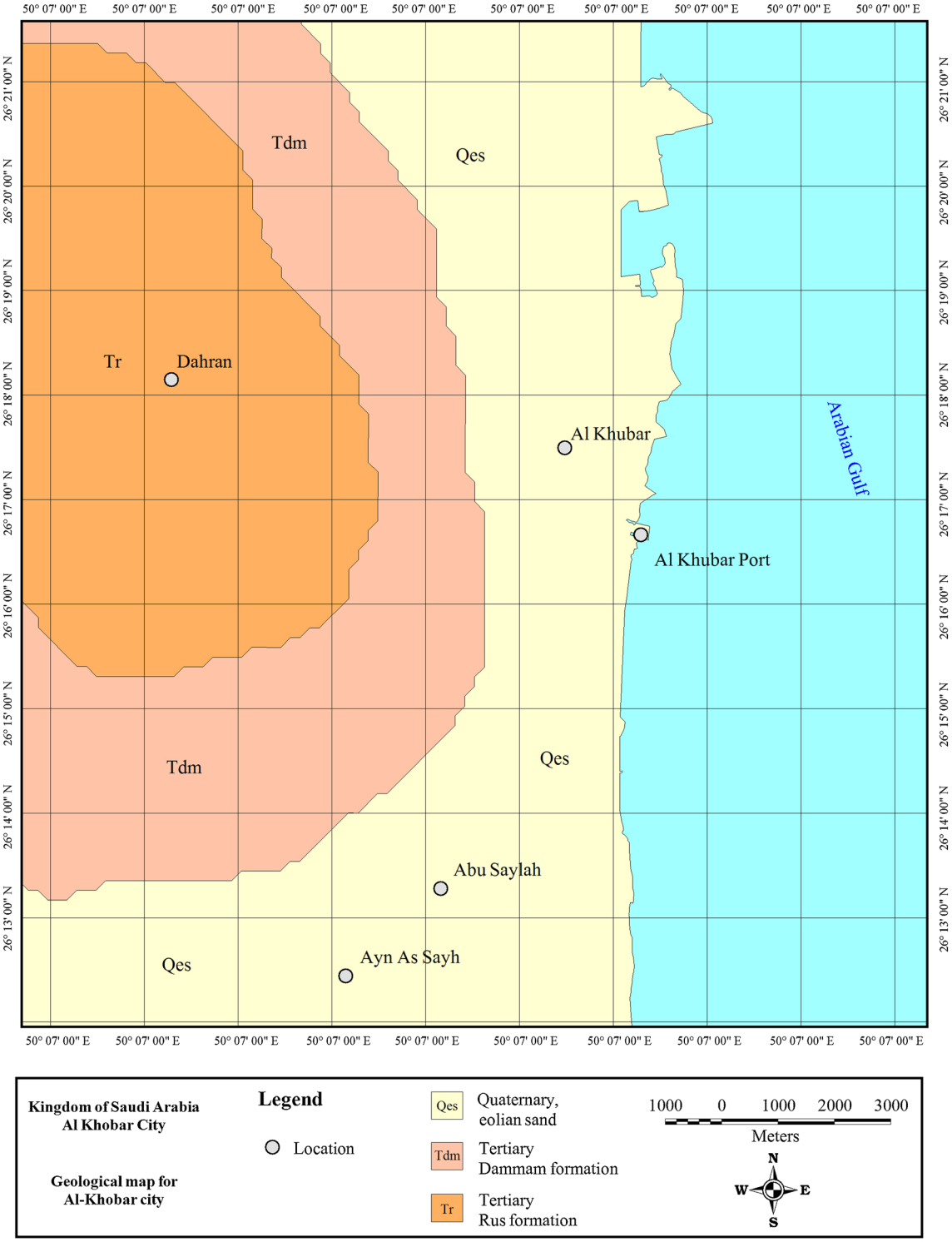

Fig. 2 Geological map of the Al Khobar area (after Saudi Geological Survey)

Site response assessment

According to Nakamura (1989), the *H*/*V* spectral ratio is a reliable estimation of the site response to S-waves, providing reliable estimates not only of the resonance frequency but also of the corresponding amplification. These ratios are much more stable than the noise spectra and they exhibit a clear peak on soft soil sites, which is well correlated with the fundamental resonance frequency. This method gained much interest because of its low-cost, rapid field operations and simple analytical procedure. Nakamura's simple model is based on the assumption that: 1) Microtremors are composed mainly of

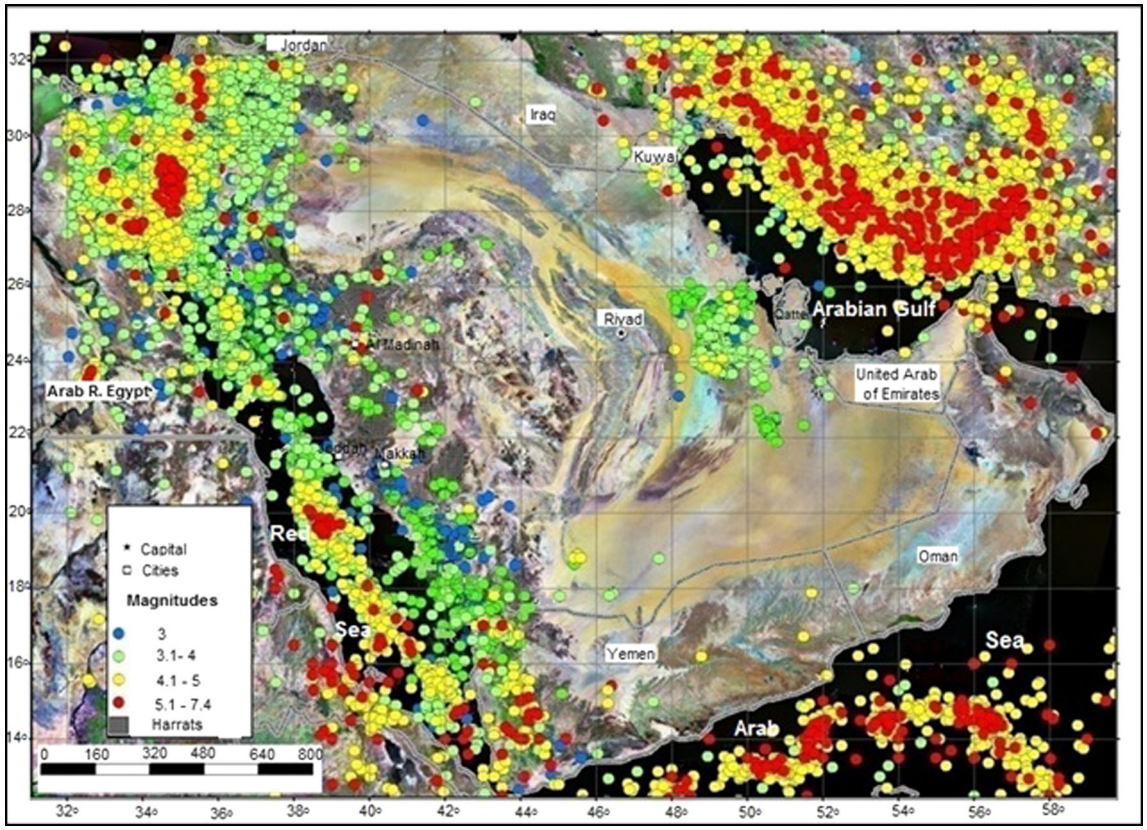

Fig. 3 Seismicity map for the Arabian Peninsula (after Saudi Geological Survey)

Rayleigh waves, propagating in soft surface layers overlying a half-space; 2) vertical motions are not affected by soft soils; 3) microtremors are originated by local surface sources (traffic and industrial noise) without any contribution from deep sources; and 4) amplification of the vertical component is exclusively associated with the depth of the surface (Rayleigh) wave's motion.

Data acquisition

Microtremor data acquisition

Al Khobar City has been divided into a grid of points with distance of 500 m×500 m as possible, each constituting a discrete measurement site. Microtremor measurements were acquired through the period from February 2010 to April 2011 during several field trips, in the quiet time intervals of the night, using a Taurus digital seismograph and Trillium compact 120 s seismometer (Nanometrics Inc., Canada). Figure 4 illustrates the locations of 113 measuring sites in Al Khobar. At each site, microtremors were recorded continuously for almost 1 h following the precautions of Nakamura (1996), Mucciarelli et al. (1998), Mucciarelli (1998), and Bard and SESAME-Team (2005). Digital records were obtained in the range of a 0.2–25-Hz band-pass filter with a sampling frequency of 100 samples per second. The length of recording is an important parameter, where a too short period will result in unreliable average spectral ratios. The sensors used were calibrated and installed in good coupling with the ground surface. Then, the sensors were oriented horizontally (north-south and east-west) and vertically leveled. Furthermore, they were isolated thermally against temperature changes using thick foam boxes, which also reduce the interference by wind.

Borehole geotechnical data

Twenty-nine geotechnical boreholes have been drilled inside Al Khobar City (Fig. 5) specifically for this project. In addition, a huge amount of geotechnical data have been collected from the General Directorate of Education in the eastern province for soil tests in Al Khobar City. Shear wave velocity is a critical factor to identify the stiffness of the sediment in determining the amplitude of ground motion (Joyner and Fumal 1984; Boore et al., 1993; Anderson et al., 1996) and might be a useful parameter to characterize local geologic conditions quantitatively for calculating site response (Park and Elrick, 1998). As an alternative, the relations between shear wave velocity and several other physical properties (i.e., the Standard Penetration Test) can be determined. These

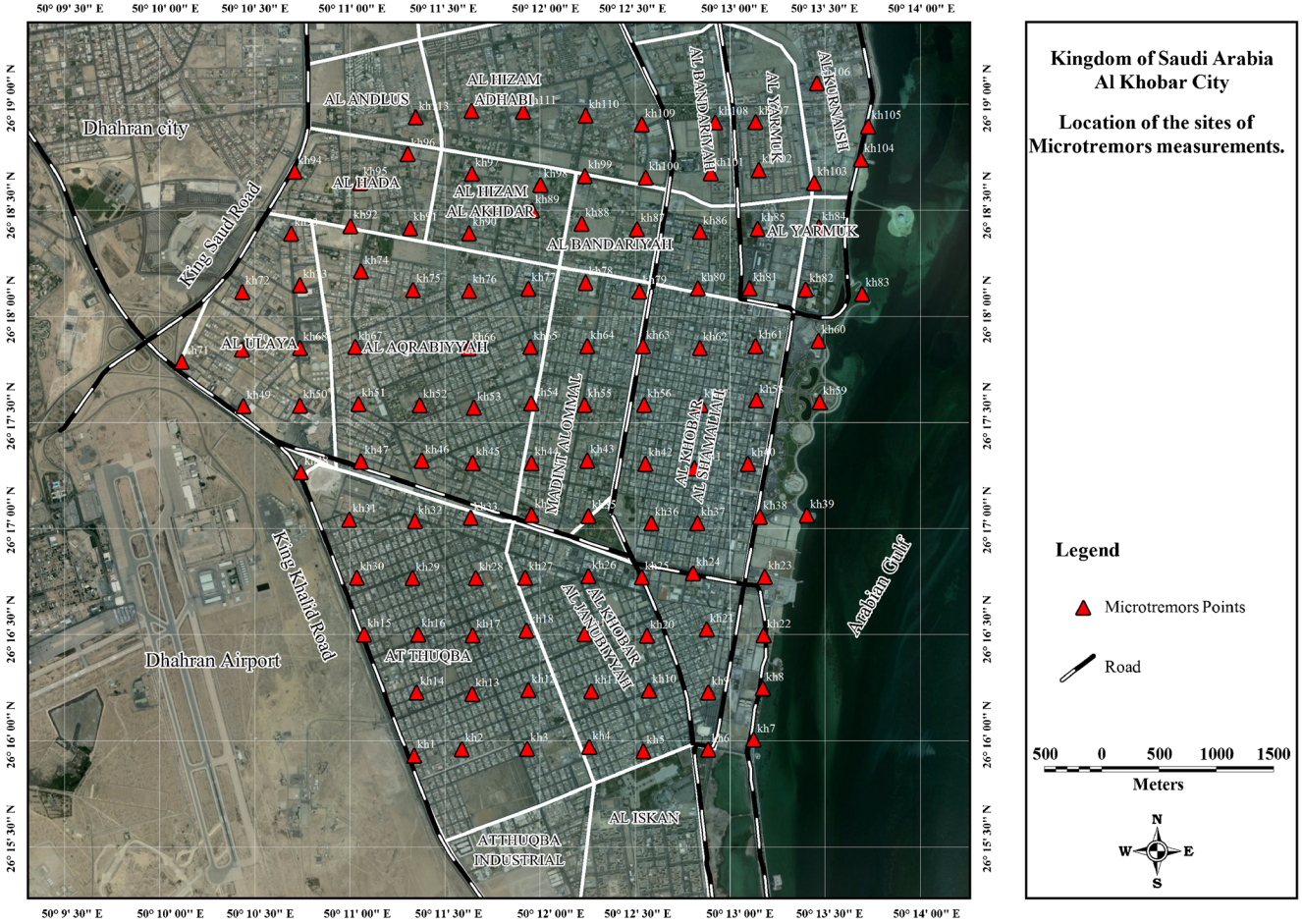

Fig. 4 Microtremor measurements in Al Khobar City

correlations can be applied to the areal distribution of physical properties and thickness of the geologic units to estimate and map shear wave velocity up to 30 m (V_{s30}), which is useful for seismic zonation studies.

Data processing and results

Microtremor measurements

The microtremor measurements were processed using the Geopsy software developed within the framework of the SESAME European project (http://www.geopsy.org/). At each site, the recorded data file was divided into several time windows of 30–50 s for spectral calculations. This length of time window has proven to be sufficiently long to provide stable results. The selected time windows were Fourier transformed using cosine tapering before transformation. The spectra were then smoothed with a Konno & Ohmachi algorithm (Konno and Ohmachi, 1998). After data smoothing, the spectra of EW and NS channels at a site were divided by the spectra of the vertical channel to get spectral ratios. The geometrical average of the two component ratios is the site amplification function. However, in most cases, due to the influence of sources like dense population, high traffic, and industrial activities, the resonance frequency cannot be directly identified from microtremor spectra (Duval et al., 2004). The estimated values of fundamental resonance frequencies and the corresponding amplifications at the measuring sites are summarized in Table 1. Figures 6 and 7 are examples of microtremor measurements.

Figure 8 illustrates the values of f_0 in Al Khobar City, which can be classified into three zones as follows: The first zone varies from 0.3 to 1.03 Hz and occupies the northeastern coastal strip, the second one ranges from 1.23 to 1.83 Hz and covers the western area, while the third one goes from 1.03 to 1.23 and is encountered in the central region. In addition, the amplification factor in Al Khobar City reached up to 2.55 (Fig. 9). The city can be separated into three zones, to some extent, according to the amplification factor. Areas with values less than 1.35 include the Al-Thuqba, Al-Andlus, Al-Hizam Al-Adhabi, Al-Hizam Al-Akhder, Albandariyah, and Al-Hada districts, and in addition the northern half of the Al-

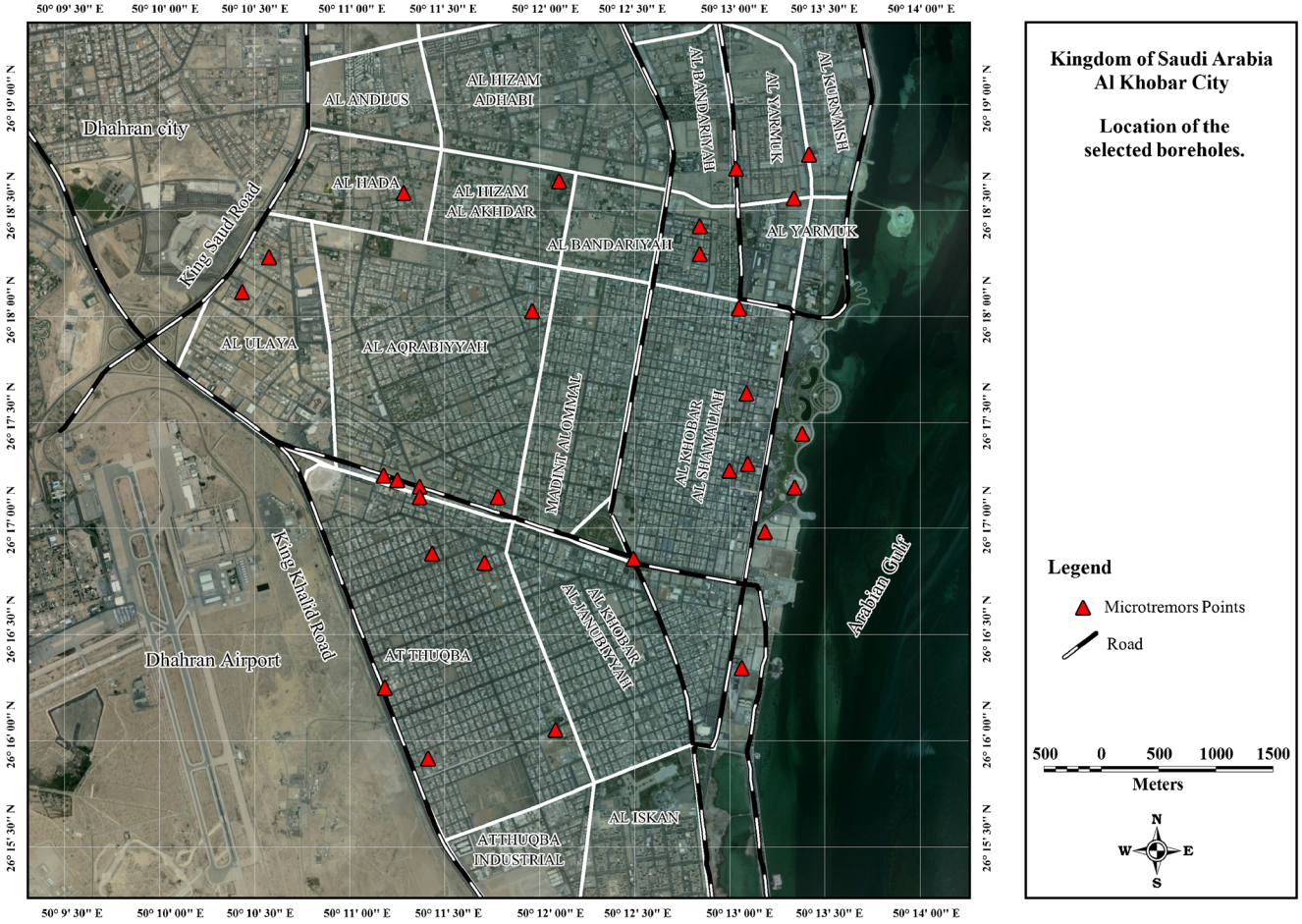

Fig. 5 Geotechnical boreholes in Al Khobar City

Aqrabiyyah, Madint Al-Ommal and Al-Khobar Al-Shamaliah districts. The second zone has A_0 in the range from 1.35 to 2, while the third zone has A_0 greater than 2 and occupies the Al-Ulaya, Al-Bustan, Al-Yarmuk, Al-Kornaish, Al-Iskan, and Al-Thuqba industrial districts.

Borehole geotechnical data

Recent seismic code provisions have been adapted for site classification, using average shear wave velocity and standard penetration results in the upper 30 m of a site as the sole parameter for site classification (Borcherdt, 1994; Borcherdt and Glassmoyer, 1994; Dobry et al., 2000). The site conditions specified by IBC 2006 are identical to the provisions of IBC 2003 and practically distinguish soil profiles in the five main categories. Each category is assigned factors appropriate for the site conditions. The average shear wave velocity and the average standard penetration resistance to 30 m [(V_s(30) and N(30)] have been calculated and then used to develop categories for local site conditions in Al Khobar using the following equations:

$$V_s(30) = \frac{\sum_{i=1}^{n} d_i}{\sum_{i=1}^{n} \frac{d_i}{v_{si}}}$$

$$N(30) = \frac{\sum_{i=1}^{n} d_i}{\sum_{i=1}^{n} \frac{d_i}{N_i}}$$

where V_{si} is the shear wave velocity (m/s), N_i is the standard penetration resistance (ASTM D 158-84) not exceeding 100 blows per 0.3 m as directly measured in the field without corrections, and d_i is the thickness of any layer between 0 and 30 m.

Table 1 Results of microtremor data analysis of Al Khobar City

Site code	No. of samples	n_w	I_w	n_c	A_0	$\sigma_A(f)$	f_0	σ_f
Kh01	180,000	13	25	328.25	1.57	1.29	01.01	0.07
Kh02	180,000	10	30	302.4	1.49	1.20	01.00	0.06
Kh03	180,000	10	40	385.2	1.64	1.22	00.96	0.05
Kh04	180,000	12	40	296.64	3.19	1.42	00.61	0.12
Kh05	180,000	10	30	303.0	1.44	1.37	01.01	0.07
Kh06	180,000	11	50	554.95	1.30	1.16	01.00	0.06
Kh07	180,000	10	50	506.5	1.20	1.19	01.01	0.07
Kh08	180,000	10	50	504.5	1.20	1.30	01.00	0.08
Kh09	180,000	10	50	438.0	1.50	1.14	00.87	0.09
Kh10	180,000	10	25	241.0	1.11	1.56	00.96	0.03
Kh11	180,000	10	25	432.5	1.11	1.35	01.73	0.09
Kh12	120,000	10	50	435.0	1.01	1.20	00.87	0.10
Kh13	120,000	14	30	427.98	0.90	1.35	01.01	0.07
Kh14	120,000	15	30	415.35	0.81	1.41	00.92	0.10
Kh15	120,000	25	40	527	2.79	0.92	1.24	0.01
Kh16	120,000	10	40	650.0	0.71	1.17	01.62	0.08
Kh17	120,000	10	20	230.4	1.09	1.35	01.15	0.24
Kh18	120,000	10	40	480.4	2.05	1.50	01.20	0.04
Kh19	120,000	12	30	292.5	1.34	1.25	00.97	0.09
Kh20	120,000	10	25	233.025	1.81	1.45	00.71	0.11
Kh21	120,000	10	30	291	1.20	1.17	00.97	0.07
Kh22	180,000	10	40	380	1.20	1.19	00.95	0.10
Kh23	180,000	10	40	348	1.08	1.18	00.87	0.07
Kh24	150,000	10	30	273	1.34	1.28	00.91	0.07
Kh25	120,000	10	40	304	1.35	1.14	0.76	0.09
Kh26	12,000	10	30	303	1.08	1.34	01.01	0.05
Kh27	89,583	10	30	321	1.07	1.27	01.07	0.08
Kh28	180,000	14	35	2314.2	1.03	1.35	00.91	0.08
Kh29	180,000	15	50	445.9	1.03	1.34	00.87	0.13
Kh30	180,000	26	50	569	3.95	1.02	01.38	0.06
Kh31	180,000	10	50	480	1.26	1.23	00.96	0.19
Kh32	120,000	10	50	480	0.92	1.23	00.96	0.15
Kh33	120,000	10	40	404	1.05	1.21	01.01	0.06
Kh34	120,000	10	30	273	1.70	1.54	00.91	0.08
Kh35	180,000	10	40	320	0.95	1.24	00.80	0.10
Kh36	120,000	10	30	273	1.30	1.37	00.91	0.08
Kh37	120,000	10	18	1160.2	2.14	1.82	00.89	0.07
Kh38	120,000	13	50	596.7	1.21	1.26	00.91	0.04
Kh39	120,000	13	50	785	1.18	1.22	01.57	0.09
Kh40	120,000	10	30	435	1.71	1.49	01.45	0.08
Kh41	120,000	10	40	1748	2.82	1.15	04.37	0.55
Kh42	120,000	10	40	592	1.42	1.23	01.48	0.06
Kh43	120,000	10	50	1980	3.95	1.11	03.96	0.40
Kh44	120,000	10	50	860	1.78	1.25	01.72	0.07
Kh45	160,000	27	50	927	3.32	1.01	01.53	0.08
Kh46	180,000	10	50	525	2.97	1.55	01.05	0.10
Kh47	120,000	10	50	490	1.46	1.16	00.98	0.17

Table 1 (continued)

Site code	No. of samples	n_w	I_w	n_c	A_0	$\sigma_A(f)$	f_0	σ_f
Kh48	120,000	10	50	200	4.76	1.30	00.40	0.05
Kh49	120,000	10	50	504	2.02	1.21	01.008	0.05
Kh50	180,000	10	50	790	3.24	1.19	01.58	0.25
Kh51	180,000	10	50	503.5	2.11	1.15	01.00	0.05
Kh52	180,000	10	50	504	1.49	1.21	01.00	0.14
Kh53	180,000	13	50	655.2	1.53	1.20	01.00	0.07
Kh54	180,000	10	50	505	0.80	1.21	01.01	0.23
Kh55	180,000	10	30	491.4	1.08	1.35	01.63	0.09
Kh56	120,000	10	30	1515	2.98	1.09	05.05	0.46
Kh57	120,000	10	30	303	1.003	1.16	01.01	0.09
Kh58	120,000	10	25	240	1.00	1.23	00.96	0.06
Kh59	120,000	10	40	1436	3.80	1.11	03.59	0.24
Kh60	160,000	28	50	870	3.29	1.26	2.68	0.17
Kh61	120,000	10	25	252.5	1.42	1.32	01.01	0.05
Kh62	150,000	19	40	248	0.98	1.50	00.62	0.09
Kh63	120,000	10	40	402	1.00	1.23	01.00	0.05
Kh64	180,000	10	50	500	0.86	1.13	01.00	0.05
Kh65	120,000	10	40	400	1.03	1.21	01.00	0.07
Kh66	180,000	10	50	910 227.5	0.88	1.28	01.82	0.09
Kh67	120,000	10	25	955	0.88	1.33	00.91	0.05
Kh68	120,000	10	50	504	1.26	1.21	01.91	0.07
Kh69	120,000	10	50	1005	1.53	1.20	01.00	0.07
Kh70	120,000	10	50	530	2.05	1.17	02.01	0.32
Kh71	120,000	10	50	505	1.17	1.13	01.06	0.08
Kh72	120,000	10	50	1000	1.32	1.16	01.01	0.06
Kh73	120,000	10	50	1455	1.72	1.23	02.00	0.48
Kh74	120,000	10	50	710	1.87	1.13	02.91	0.28
Kh75	160,000	25	50	864	3.29	1.02	2.82	0.07
Kh76	120,000	10	40	652	1.07	1.19	01.63	0.06
Kh77	180,000	10	50	675	1.11	1.11	01.35	0.06
Kh78	180,000	10	50	435	1.02	1.21	00.87	0.08
Kh79	120,000	10	50	500	1.21	1.20	01.00	0.05
Kh80	120,000	10	50	475	1.10	1.28	00.95	0.07
Kh81	120,000	10	50	1555	3.26	1.26	03.11	0.39
Kh82	120,000	16	35	560	1.45	1.35	01.00	0.03
Kh83	180,000	10	40	404	1.55	1.30	01.01	0.05
Kh84	120,000	10	30	1134	4.71	1.35	03.78	0.43
Kh85	120,000	10	40	1300	02.91	1.21	03.25	0.44
Kh86	120,000	10	40	1304	2.79	1.16	03.26	0.16
Kh87	180,000	10	50	530	1.04	1.22	01.06	0.07
Kh88	180,000	10	50	450	0.96	1.23	00.90	0.05
Kh89	120,000	20	50	1650	0.88	1.15	01.65	0.06
Kh90	120,000	30	50	1549	3.19	1.21	1.94	0.09
Kh91	120,000	10	50	825	1.10	1.20	01.65	0.06
Kh92	120,000	10	50	580	0.91	1.17	01.16	0.09
Kh93	120,000	10	50	610	1.53	1.21	01.22	0.05
Kh94	120,000	10	50	860	1.06	1.20	01.72	0.09
Kh95	120,000	10	50	505	1.11	1.11	01.01	0.09

Table 1 (continued)

Site code	No. of samples	n_w	I_w	n_c	A_0	$\sigma_A(f)$	f_0	σ_f
Kh96	180,000	10	50	505	1.21	1.19	01.01	0.05
Kh97	120,000	10	50	405	1.08	1.23	00.81	0.09
Kh98	120,000	10	50	400	0.87	1.21	00.80	0.07
Kh99	120,000	10	20	180	1.28	1.44	00.90	0.10
Kh100	120,000	10	50	575	0 1.17	1.16	01.15	00.61
Kh101	120,000	10	50	580	0.99	1.25	01.16	0.09
Kh102	180,000	10	30	363	1.18	1.27	01.21	0.31
Kh103	180,000	12	50	1770	2.67	1.24	03.25	0.11
Kh104	120,000	10	30	273	1.08	1.33	00.91	0.42
Kh105	120,000	29	50	837	3.59	1.12	3.09	0.10
Kh106	120,000	10	50	2530	2.50	1.29	05.06	0.55
Kh107	120,000	10	40	1300	3.37	1.15	03.25	0.43
Kh108	120,000	10	50	1865	2.72	1.10	03.73	0.33
Kh109	120,000	10	40	700	1.15	1.32	01.75	0.07
Kh110	120,000	10	15	148.5	1.13	1.69	00.99	0.08
Kh111	180,000	10	50	500	0.98	1.30	01.00	0.10
Kh112	120,000	10	50	505	1.49	1.22	1.72	0.03
Kh113	120,000	25	50	769	2.98	1.19	2.16	0.06

I_w window length, n_w number of windows selected for the average H/V curve, $n_c=I_w\ n_w\ f_0$ the number of significant cycles, A_0 H/V peak amplitude at frequency f_0, $\sigma_A(f)$ "standard deviation" of $A_{H/V}$ (f), f_0 H/V peak frequency, σ_f standard deviation of H/V peak frequency ($f_0 \pm \sigma_f$)

Standard penetration test values have been corrected to compensate for the field testing procedure (Skempton, 1986) according to the following equation:

$$N_{60} = 1.6 E_m C_b C_r N$$

where

N_{60}=standard penetration test N value corrected for field testing procedures; E_m=hammer efficiency (for US equipment, E_m is 0.6 for a safety hammer and 0.45 for a doughnut hammer); C_b=borehole diameter correction (C_b=1.0 for boreholes of 65–115-mm-diameter, 1.05 for 150-mm-diameter, and 1.15 for 200-mm-diameter holes); C_r=rod length correction (C_r=0.75 for up to 4 m of drill rods, 0.85 for 4 to 6 m of drill rods, 0.95 for 6 to 10 m of drill rods, 1.0 for drill rods in excess of 10 m); and N= measured standard penetration test N value.

After this procedure, the average shear wave velocity has been calculated using the Boore (2004) equation:

$$V_s\,(30) = {}^{30}\!/_{(tt(d)+\,(30-d)/v_{eff})}$$

where V_{eff} is the assumed effective velocity from depth d to 30 m. Then, the fundamental frequency values (f_0) can be estimated at each borehole (Fig. 10 and Table 2) based on the following equation:

$$F_0 = \frac{\beta_1}{4h}$$

where β_1=the shear wave velocity in the surficial layer and h=the thickness of the surficial layer. Figure 11 presents the depth of bedrock (h) through Al Khobar City from geotechnical boreholes.

The ground motion amplitudes (A_0) are then calculated (Fig. 12) using the equation of Borchert et al. (1991) as follows:

$$\mathrm{AHSA} = 700/V_1$$

where AHSA is the average horizontal spectral amplification and V_1 is the average shear wave velocity down to a depth of 30 m (m/s).

Discussions and conclusions

One hundred twelve microtremor measurements were acquired at grid points in the densely populated city

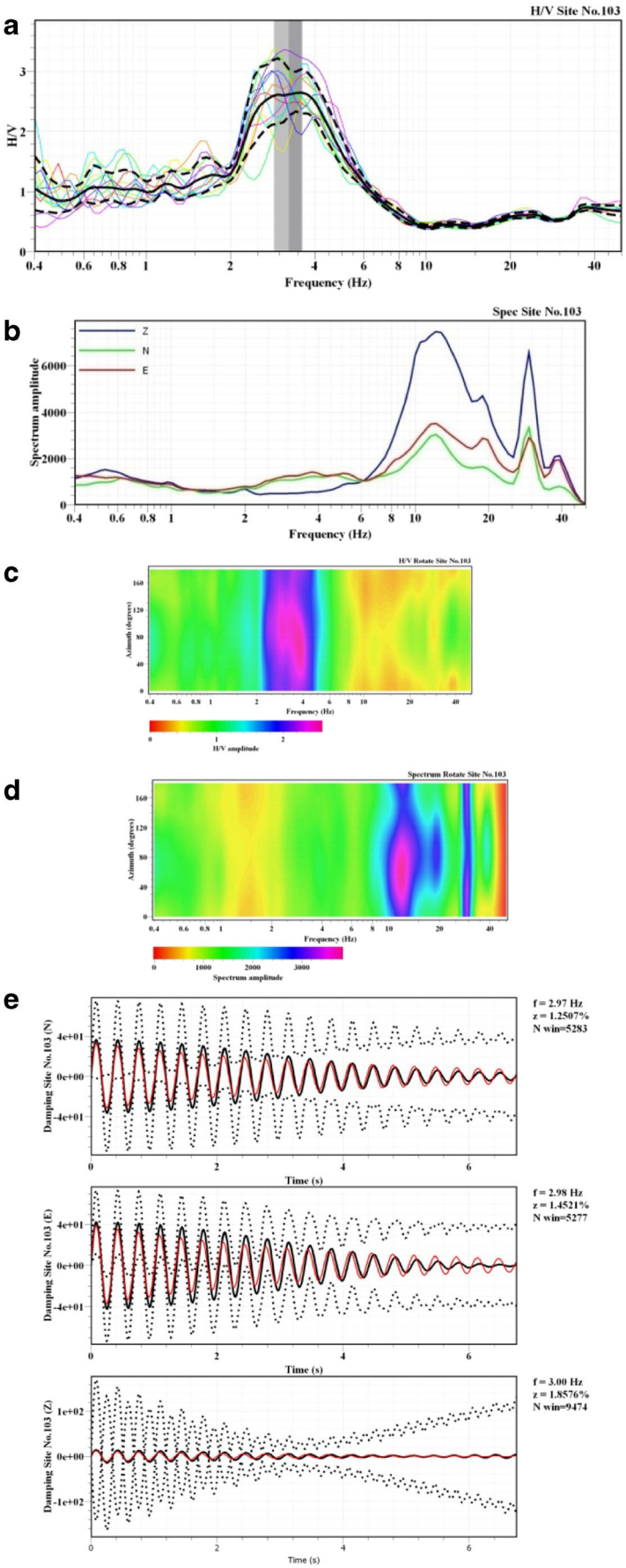

Fig. 6 Results of site no. 103 (as example) where **a** demonstrates the *H*/*V* spectral ratio curve, **b** represents the amplitude spectrum of the three comp., **c** illustrates the *H*/*V* rotation with azimuth degrees, **d** shows the horizontal spectrum rotation with azimuth degrees, **e** shows the damping test for the peak amplitude of natural origin

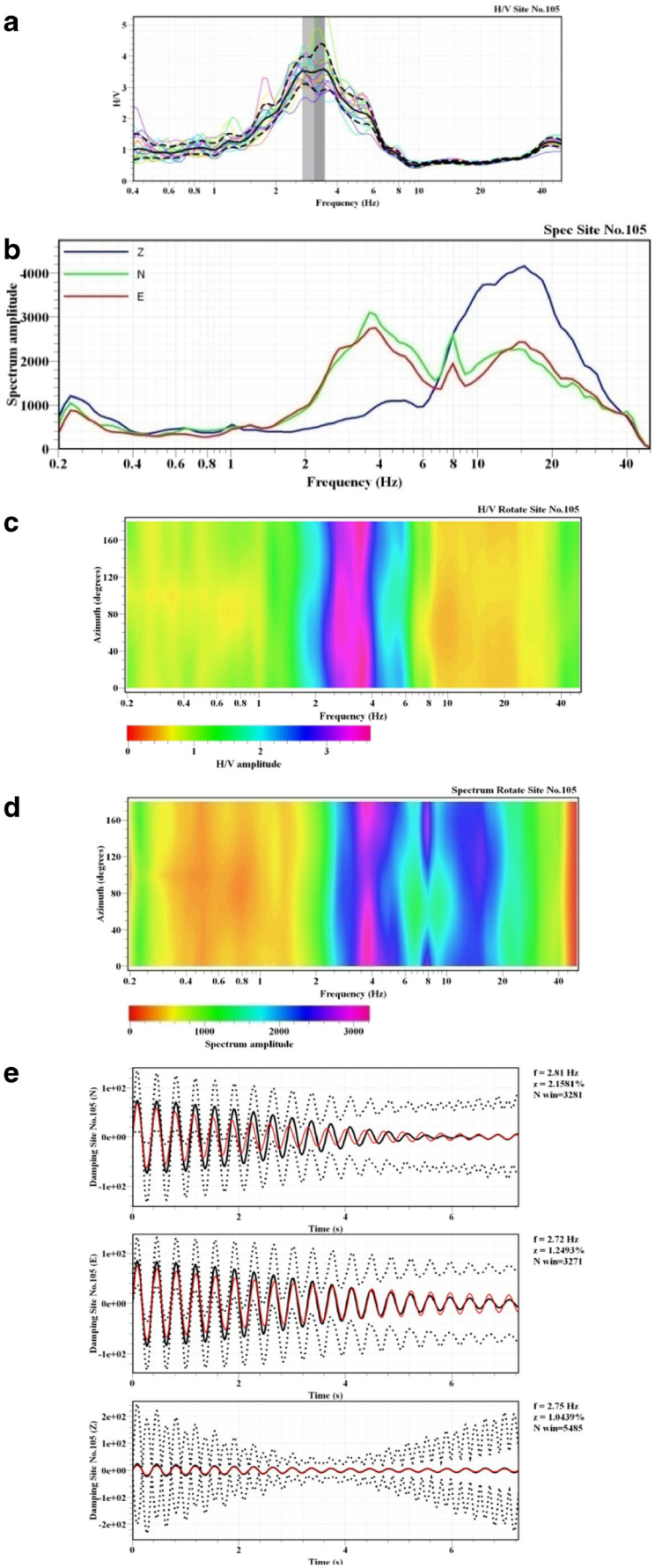

Fig. 7 Results of site no. 105 (as example) where **a** demonstrates the *H*/*V* spectral ratio curve, **b** represents the amplitude spectrum of the three comp., **c** illustrates the *H*/*V* rotation with azimuth degrees, **d** shows the horizontal spectrum rotation with azimuth degrees, **e** shows the damping test for the peak amplitude of natural origin

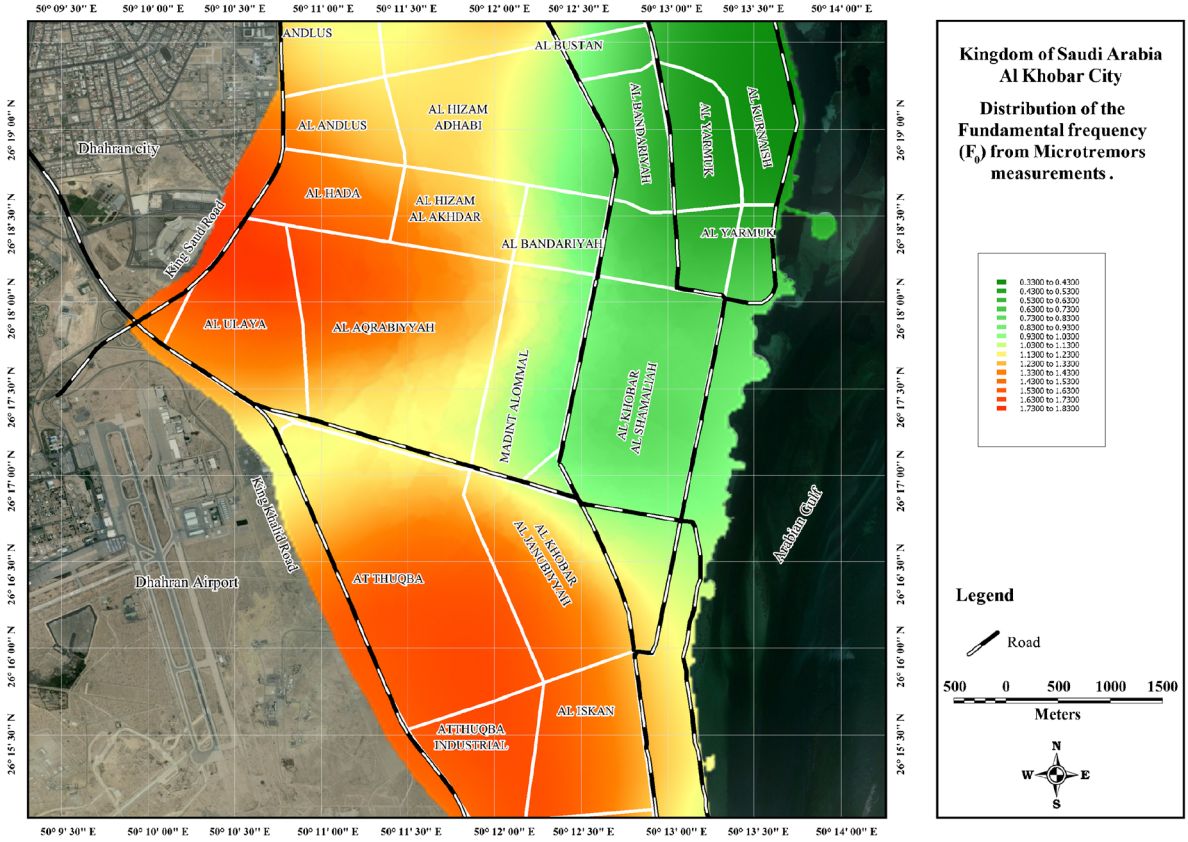

Fig. 8 Distribution of the fundamental frequencies (f_0) in Al Khobar City

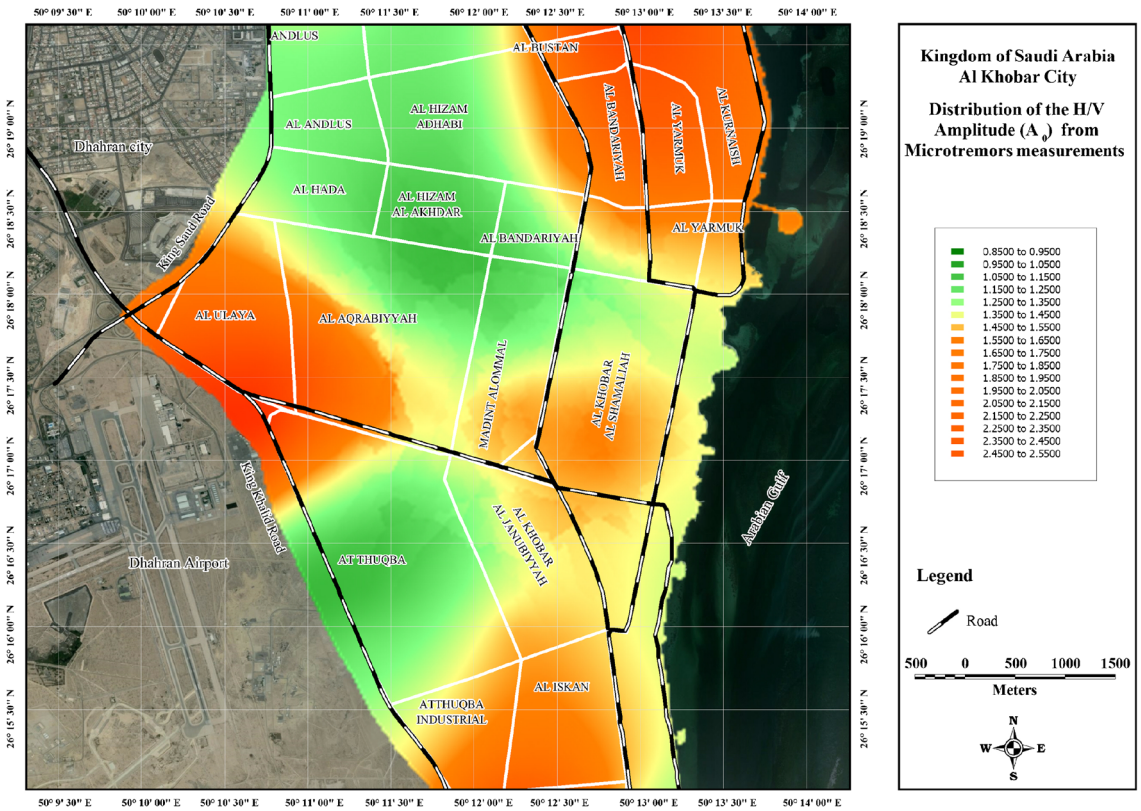

Fig. 9 Distribution of the amplification factor (A_0) in Al Khobar City

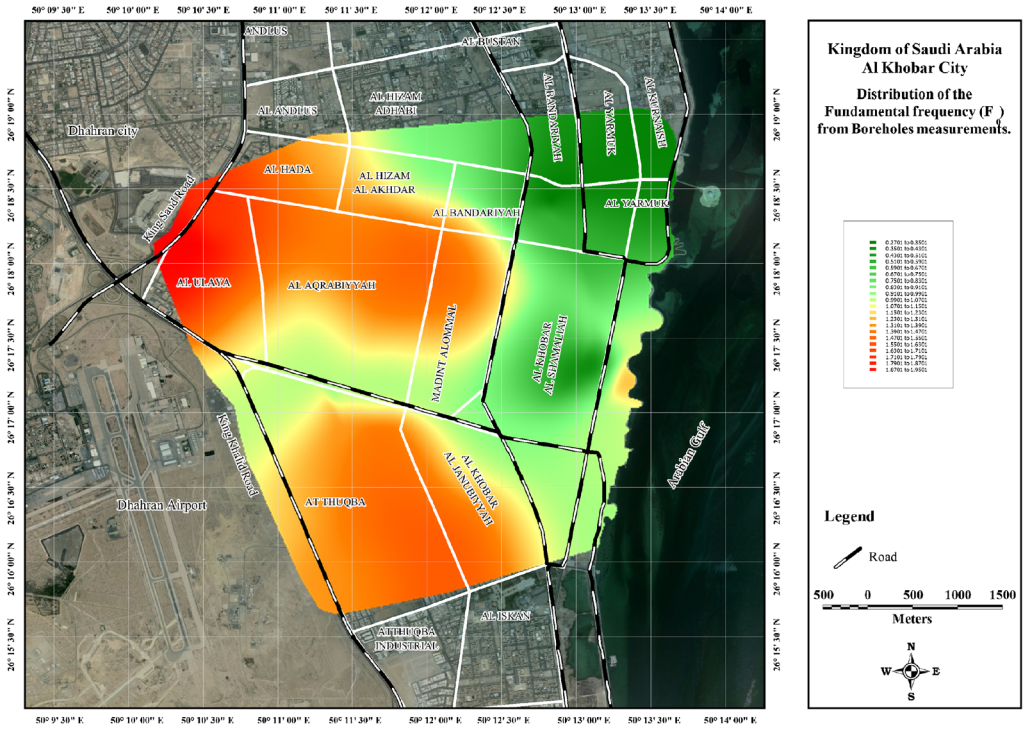

Fig. 10 Distribution of f_0 based on borehole data

Table 2 Results of the geotechnical borehole data in Al Khobar City

No. of borehole	V_{av}	V_{30}	T_0 (s)	f_0 (Hz)	A_0
BH01	136	236	0.76	1.32	1.40
BH02	300	366	0.65	1.53	1.61
BH03	160	171	0.8	1.25	1.20
BH04	88	153	1.05	0.95	1.27
BH05	222	229	0.73	1.4	1.04
BH06	125	236	1.17	0.9	1.28
BH07	250	277	0.81	1.3	0.94
BH08	308	345	1.02	0.97	1.31
BH09	500	577	1.01	0.98	1.97
BH10	375	405	1.03	0.96	1.66
BH11	375	379	1.01	0.98	1.87
BH12	303	326	1.01	0.98	1.72
BH13	161	150	1.06	0.96	1.18
BH14	108	152	3.37	0.35	2.00
BH15	118	121	1.22	1.2	1.22
BH16	82	136	3.2	0.34	1.62
BH17	95	154	1.25	1.01	1.08
BH18	66	106	1.23	0.82	1.08
BH19	242	303	0.69	1.49	1.06
BH20	327	492	0.52	1.95	1.68
BH21	214	268	0.61	1.73	1.58
BH22	87	122	2.4	0.53	1.40
BH23	66	140	2.85	0.51	1.63
BH24	104	167	3.8	0.27	1.89
BH25	241	268	1.17	0.86	1.02
BH26	204	236	0.82	1.29	1.13
BH27	120	129	3.61	0.3	1.59
BH28	94	116	3.28	0.32	1.69
BH29	96	142	3.73	0.29	1.92

V_{av} average shear wave velocity, T_0 natural period, f_0 fundamental frequency, A_0 relative amplification

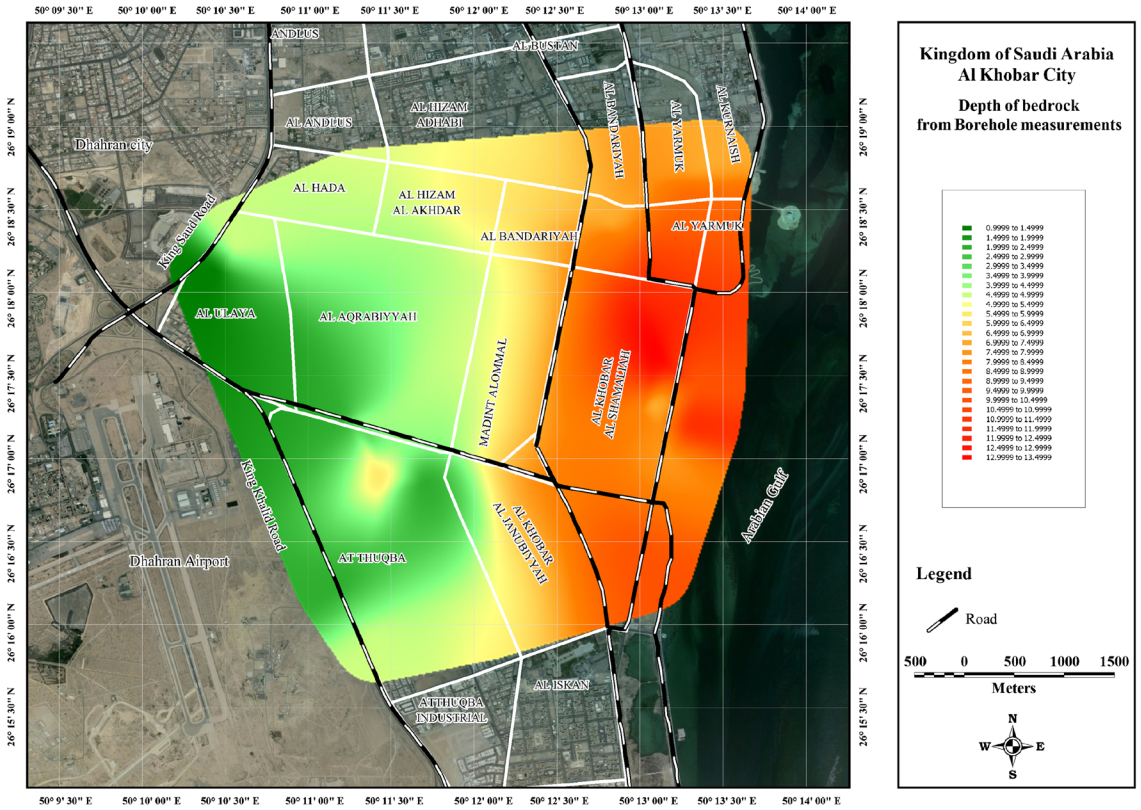

Fig. 11 Depth to bedrock in Al Khobar City based on borehole data

of Al Khobar. From these measurements, the horizontal-to-vertical spectral ratios were obtained following the Nakamura technique, which proved to be a valuable tool to determine the distribution of areas with large and small thickness of soft soils. From borehole data, the resonance frequency and amplitude spectral ratios were calculated.

Furthermore, the fundamental resonance frequencies determined in the present study are correlated well with the thickness of unconsolidated sediments in Al Khobar City. These sediments are thick in the northern part (where site response spectra exhibit peaks at 0.33–1.03 Hz), whereas they are thin in the southern part of the city (predominant frequency of site response at 1.23–1.73 Hz). This behavior indicates horizontal variations both in the thickness and type of sediments. A good correlation has also been observed between the microtremor and borehole results, both in terms of fundamental frequencies and amplification levels (Table 2).

The obtained amplification values are in agreement with the surface geology of the study area, where the higher H/V values occupy the northern part of Al Khobar due to the presence of coastal deposits and sabkha sediments. The lower values are encountered in the southern parts of the city. This variation in the H/V values also reflects variation in sediment thickness.

The relationship between the height of a building and its fundamental period of vibration can be expressed as T=(number of stories)/10. It can be expected that in this urban area the natural frequency of the soil corresponds to the frequency of buildings with ≥1 story. Site response frequencies less than 10 Hz are of engineering concern for one story reinforced concrete structures. Fundamental frequencies in the range between 0.33 and 1.73 Hz prevail in Al Khobar City, which means that in this urban area the natural frequency of the soil corresponds only to the fundamental frequency of buildings with ≥5 stories.

However, according to Parolai et al. (2006), when the fundamental frequency of the vibration of a building is higher than that of the fundamental frequency of the soil, f_0, it may be close to the frequency of higher modes. Higher modes are expected at frequencies $f_n=(2n+1)f_0$, where n=1, 2, 3,…, and f_0 is the fundamental frequency. The H/V spectral ratio provides the lower frequency threshold from which ground motion amplification due to soft soil can be expected. Therefore, one cannot exclude that in the Al Khobar

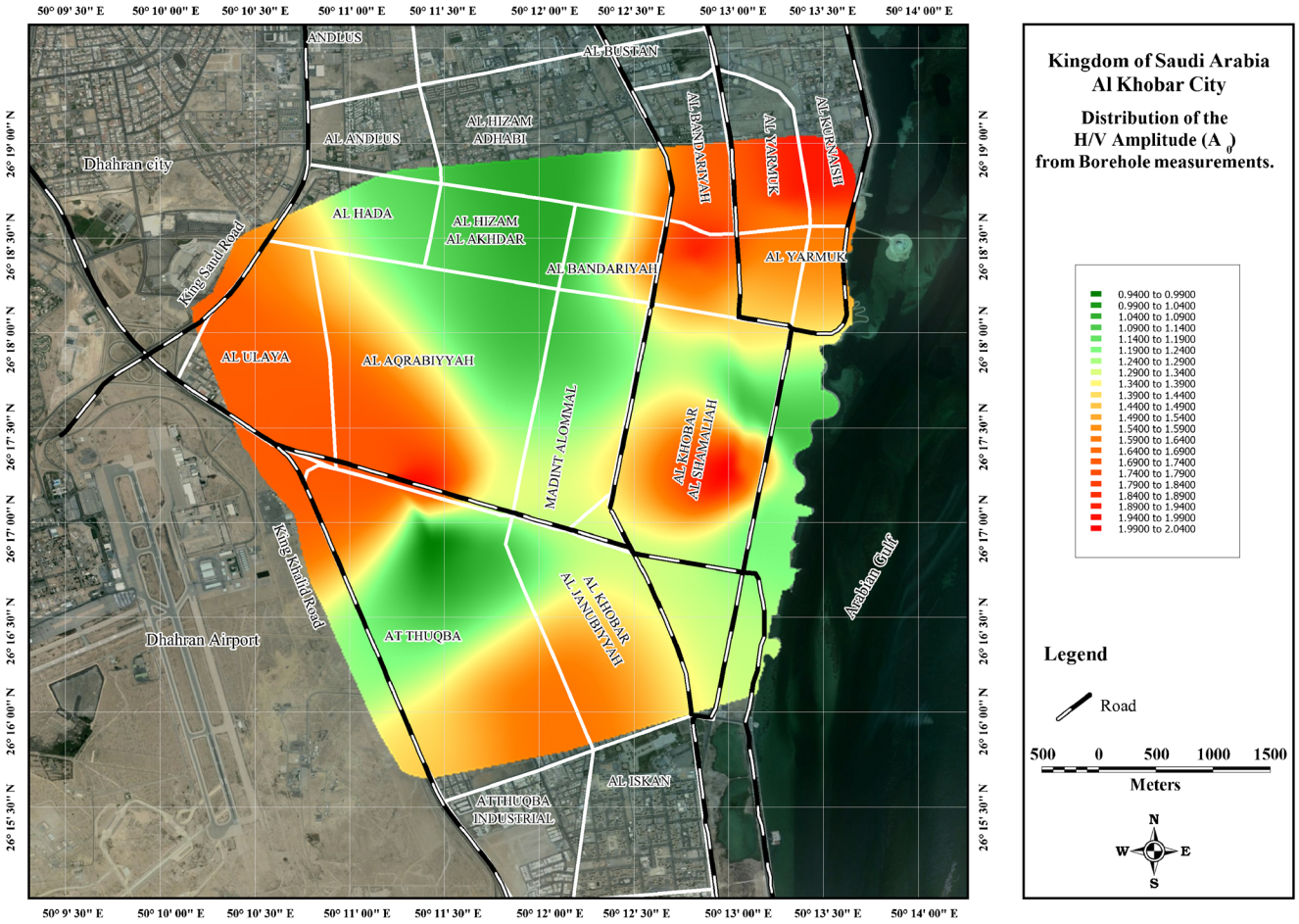

Fig. 12 Distribution of A_0 from borehole data

urban area soil amplification of ground motions may also occur at higher mode frequencies close to the fundamental frequency of vibration of low-rise buildings, even if it is smaller than that at the fundamental frequency of the sedimentary cover. These results strongly highlight the need for a seismic hazard assessment in the eastern part of Saudi Arabia.

Acknowledgments This project was funded by the National Plan for Science, Technology and Innovation (MAARIFAH), King Abdulaziz City for Science and Technology, Kingdom of Saudi Arabia, Award Number (08-SPA239-2).

References

Al-Amri A, Rodgers A, Al-khalifah T (2008) Improving the level of seismic hazard parameter in Saudi Arabia using earthquake location. Arab J Geosci 1:1–15. doi:10.1007/s12517-008- 0001-5

Al-Malki M, Fnais M, Al-Amri A, Abdelrahman K (2014) Estimation of fundamental frequency in Dammam City. Eastern Saudi Arabia Arab J Geosci. doi:10.1007/s12517-014-1337-7

Al-Sayari SS, Zoetl JG (eds) (1978) Quaternary period in Saudi Arabia. 1. Sedimentological, hydrogeological hydrochemical, geomorphological and climatological investigations in central and eastern Saudi Arabia. Springer- Verlag, Vienna

Al-Shaabi SF (2004) Induced seismicity at Ghawar hydrocarbon reservoir, eastern Saudi Arabia. Ann Geol Surv Egypt V(XXVII):335–342

Ambraseys A (1988) Seismicity of Saudi Arabia and adjacent areas. Report 88/11, ESEE, Imperial Coll. Sci. Tech., 88/11, London, U.K

Anderson JG, Lee Y, Zeng Y, Day S (1996) Control of strong motion by the upper 30 meters. Bull Seismol Soc Am 86(6):1749–1759

Bard PY, Tucker BE (1985) Underground and ridge and site effects: comparison of observation and theory. Bull Seismol Soc Am 75: 905–922

Bard PY (2000) International training course on: seismology, seismic data analysis, hazard assessment and risk mitigation, Potsdam, Germany, 01 October to 05 November 2000

Bard PY, SESAME-Team (2005) Guidelines for the implementation of the H/V spectral ratio technique on ambient vibrations—measurements, processing and interpretations. SESAME European research project EVG1-CT-2000-00026 D23.12. Available online at http://sesame-fp5.obs.ujf-grenoble.fr.

Boore DM, Fumal TEJWB (1993) Estimation of response spectra and peak acceleration from western North American earthquakes: an interim report. US Geol Surv Open-File Rep 93–509:72

Boore DM (2004) Estimating V_{s30} (or NEHRP site classes) from shallow velocity models (depths<30 m). BSSA 94:591–597

Borcherdt R, Glassmoyer G (1992) On the characteristics of local geology and their influence on the ground motions generated by the Loma Prieta earthquake in the San Francisco bay region, California. Bull Seismol Soc Am 82:603–641

Borcherdt RD (1994) Estimates of site-dependent response spectra for design (methodology and justification). Earthquake Spectra 10: 617–653

Borcherdt RD, Glassmoyer G (1994) Influences of local geology on strong and weak ground motions in the San Francisco Bay region and their implications for site-specific building-code provisions. In: Borcherdt, R.D. (ed.): The Loma Prieta, California, earthquake of 17 October 1989—strong ground motion. US Geological Survey Prof. Pap. 1551-A-:77–108

Doherty R, Borcherdt RD, Crouse CB, Idriss IM, Joyner WB, Martin GR, Power MS, Rinne EE, Seed RB (2000) New site coefficients and site classification system used in recent building seismic code provisions. Earthquake Spectra 16:41–67

Duval AM, Chatelain JL, Guillier B, SESAME Project WP02 Team (2004) Influence of experimental conditions on H/V determination using ambient vibrations (noise). Proceedings of the 13th World Conference on Earthquake Engineering, Vancouver, August 2004, paper # 306

Field EH, Jacob KH (1995) A comparison and test of various site-response estimation techniques, including three that are not reference-site dependent. Bull Seismol Soc Am 85:1127–1143

Fnais MS, Hassanein KA-R, Al-Amri AM (2010) Microtremor measurements in Yanbu city of western Saudi Arabia: a tool of seismic microzonation. J King Saud Univ- Sci (ElSEVIER). doi:10.1016/j.jksus.2010.02.006

Jackson JA, Fitch T (1981) Basement faulting and the focal depths of the larger earthquakes in the Zagros Mountains (Iran). Geophys J R Astron Soc 64:562–586

Joyner WB, Fumal TE (1984) Use of measured shear-wave velocity for predicting geologic and site effects on strong ground motion. Proc 8th world Conf Earthquake Eng 2:777–784

Konno K, Ohmachi T (1998) Ground-motion characteristics estimated from spectral ratio between horizontal and vertical components of microtremors. Bull Seismol Soc Am 88:228–241

Lachet C, Bard PY (1994) Numerical and theoretical investigations on the possibilities and limitations of the Nakamura's technique. J Phys Earth 42:377–397

Malagnini L, Tricarico P, Rovelli A, Herrmann RB, Opice S, Biella G, de Franco R (1996) Explosion, earthquake, and ambient noise recording in a Pliocene sediment-filled valley: inferences on seismic response properties by reference- and non-reference-site techniques. Bull Seismol Soc Am 86:670–682

Mucciarelli M (1998) Reliability and applicability of Nakamura's technique using microtremors: an experimental approach. J Earthq Eng 4:625–638

Mucciarelli M, Contri P, Monachesi G, Calvano G (1998) Towards an empirical method to instrumentally assess the seismic vulnerability of existing buildings. Proceedings of Conference on Disaster Mitigation and Information Technology, London

Nakamura Y (1989) A method for dynamic characteristics estimation of subsurface using microtremor on the ground surface. QR of RTRI 30(1):25–33

Nakamura Y (1996) Real-time information systems for hazards mitigation. Proceedings of the 11th World Conference on Earthquake Engineering, Acapulco, Mexico

Park S, Elrick S (1998) Predictions of shear wave velocities in southern California using surface geology. Bull Seismol Soc Am 88:677–685

Parolai S, Bormann P, Milkereit C (2006) Measurements of the fundamental resonance frequency of the sedimentary cover in the Cologne area: contribution to the seismic microzonation. Ergeb Dtsch Forschung Naturkat 301–305

Powers LF, Ramirez LF, Redmond CD, Elberg EL (1963) Geology of the Arabian Peninsula—sedimentary geology of Saudi Arabia. ARAM CO-USGS, 147 p

Safak E (1997) Models and methods to characterize site amplification from a pair of records. Earthquake Spectra 13:97–129

Skempton AW (1986) Standard penetration test procedures and the effects in sands of overburden pressure, relative density, particle size, aging and overconsolidation. Geotechnique 36(3):425–447

Wakamatsu K, Yasui Y (1996) Possibility of estimation for amplification characteristics of soil deposits based on ratio of horizontal to vertical spectra of microtremors. Proceedings of the 11th World Conference on Earthquake Engineering Acapulco. Mexico. Geophys Prospect 30:55–70